


## Development of an Improved Process for Doxercalciferol via a Continuous Photochemical Reaction

Bruce G. Anderson,<sup>†</sup> William E. Bauta,\* and William R. Cantrell, Jr.<sup>‡</sup>

Genzyme Corporation, 14805 Omicron Drive, San Antonio, Texas 78245, United States

 Supporting Information

**ABSTRACT:** Doxercalciferol (1 $\alpha$ -hydroxyvitamin D<sub>2</sub>) is a commercially approved vitamin D derivative used to treat chronic kidney disease (CKD) patients whose kidneys cannot metabolically introduce a hydroxyl group at C1. A new process for the production of doxercalciferol from ergocalciferol was developed using a continuous photoisomerization of a known vitamin D intermediate as the key step, thus circumventing the limitations of batch photoisomerization processes. Doxercalciferol is produced in an overall yield of about 10% from ergocalciferol.

**INTRODUCTION**

In healthy humans, dietary vitamin D<sub>2</sub> (ergocalciferol, **1**) undergoes two metabolic oxidations to afford the physiologically active form of vitamin D<sub>2</sub> (1 $\alpha$ ,25-dihydroxyvitamin D<sub>2</sub>, **2**) (Figure 1).<sup>1</sup> Oxidation at carbon 25 occurs in liver microsomes by the action of vitamin D 25-hydroxylase, whereas introduction of the 1 $\alpha$ -hydroxyl group is achieved in the kidney by 25-hydroxyvitamin D<sub>3</sub> 1 $\alpha$ -hydroxylase.<sup>2</sup> In patients with chronic kidney disease (CKD), failure to undergo normal oxidation at position 1 $\alpha$  results in a variety of detrimental health effects.<sup>3</sup> To circumvent this metabolic deficiency, 1 $\alpha$ -hydroxyvitamin D<sub>2</sub>, doxercalciferol (**3**), the active ingredient in the drug Hecitorol, which already contains the 1 $\alpha$ -hydroxyl group that would normally be introduced in the kidney, is used in the treatment of patients with moderate to severe CKD, including patients with end-stage renal disease receiving dialysis.<sup>4</sup> Given that doxercalciferol is clinically active at microgram doses and that the annual demand is less than 1 kg, it is a salient example of a high-value, low-volume, active pharmaceutical ingredient.

Various synthetic approaches to vitamin D structures are documented in the chemical literature.<sup>5</sup> Although the synthesis of doxercalciferol (**3**) from commercially available ergocalciferol (**1**) involves the introduction of a single allylic hydroxyl group, this transformation is encumbered by multiple obstacles, including competing reactivity at other allylic positions and the inherent resistance of position 1 to direct oxidation by selenium reagents, which is believed to result from unfavorable steric and conformational factors.<sup>6</sup> The problem of C1 oxidation has been addressed by different approaches involving modification of the triene moiety in a manner that masks competitive sites of reactivity and modifies the steric environment at C1. In one approach, the cyclovitamin route originally developed by Paaren and DeLuca,<sup>6,7</sup> the triene is modified via internal displacement of the carbinol at C3 as its tosylate to afford cyclovitamin (**4**) and subsequent oxidation at C1 to the carbinol (**5**) with selenium dioxide (Scheme 1). Solvolytic cycloreversion and purification then affords **3**. This approach was successfully applied to the synthesis of doxercalciferol. An alternative that has been used in related vitamin D molecules is

the sulfur dioxide approach, in which the triene is isomerized via a sulfur dioxide cycloadduct. Application to doxercalciferol would thus entail synthesis of the cycloadduct **6** from ergocalciferol (**1**) and SO<sub>2</sub>. Protection of the hydroxyl and thermal retrocycloaddition would afford the isomeric triene (**7**), which could be cleanly oxidized at C1 with selenium dioxide and protected to triene (**8**). This then would be photochemically isomerized and the alcohols deprotected to yield doxercalciferol (**3**).<sup>8</sup>

In our experience with the cyclovitamin route, a number of byproducts required removal through multiple and laborious normal phase chromatography steps. These included the *cis*-1 $\beta$ -hydroxyvitamin D<sub>2</sub> (**9**) and the *trans*-1 $\alpha$ -hydroxyvitamin D<sub>2</sub> (**10**) (Figure 2). Byproduct **9** is derived from nonstereospecific oxidation of **4**, whereas **10** results from lack of selectivity in the cyclopropane opening. Alternative purification approaches for the cyclovitamin route have included the photoisomerization of **10** to **3**,<sup>7,9</sup> and the selective Diels–Alder cycloaddition of the undesired *trans*-isomer with maleic anhydride<sup>10</sup> in order to facilitate chromatographic purification.

Owing to the difficulties we encountered with the cyclovitamin route, we turned our attention to the sulfur dioxide route and its inherent obstacle of batch photoisomerization, which is typically conducted with an immersion lamp in a cylindrical reactor. The key problem with batch photoreactors from a process standpoint is that the reaction occurs very close to the light source, with most of the batch being unaffected at a given time. As volume increases this limitation decreases efficiency, especially when mixing is not optimal. Longer reaction times and increased levels of impurities may result under such a scenario. In order to circumvent this obstacle, we investigated the application of a continuous flow isomerization reactor for the conversion of **10** to doxercalciferol (**3**) using a flow photoreactor apparatus adapted from that reported by Hook et al.<sup>11</sup> Flow photochemical processes have been reported by several groups.<sup>7,12</sup> The advantages of continuous

**Special Issue:** Continuous Processes 2012**Received:** December 1, 2011**Published:** January 29, 2012

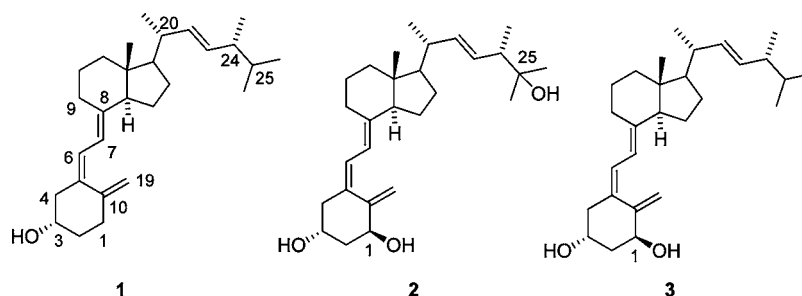
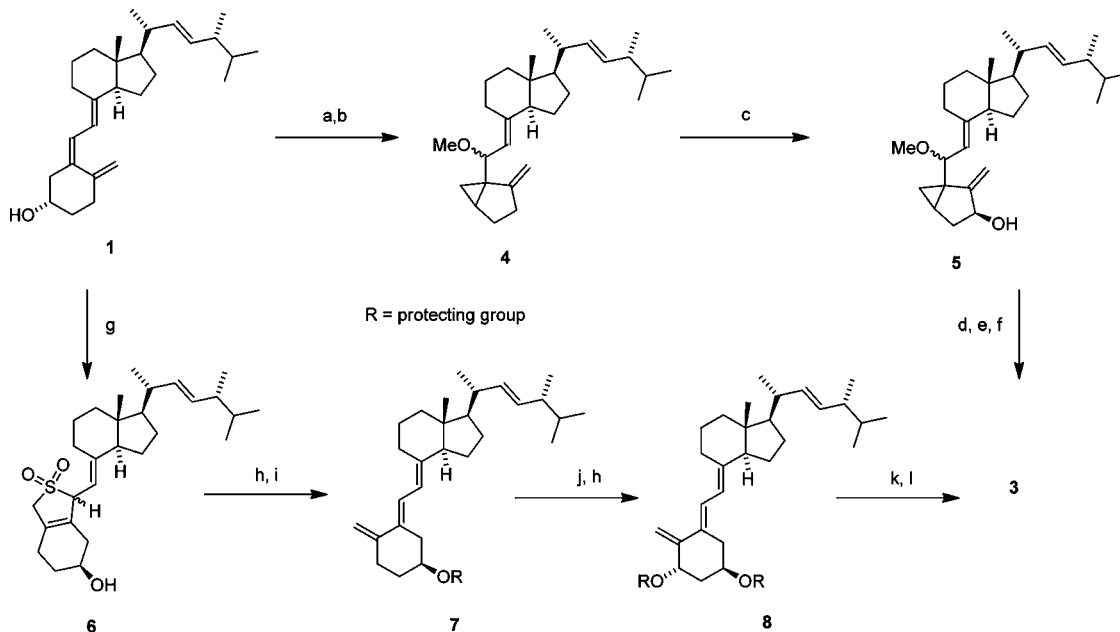


Figure 1.

Scheme 1. Synthesis of doxercalferol (3) using the cyclovitamin and sulfur dioxide routes.<sup>a</sup>



<sup>a</sup>Reaction conditions and reagents: a) TsCl, pyridine; b) NaHCO<sub>3</sub>, MeOH; c) SeO<sub>2</sub>, *t*-BuOOH, CH<sub>2</sub>Cl<sub>2</sub>; d) Ac<sub>2</sub>O, pyridine; e) H<sup>+</sup>, H<sub>2</sub>O; f) NaOH, EtOH. g) SO<sub>2</sub>; h) protection of hydroxyl group; i); NaHCO<sub>3</sub>, EtOH, heat j) SeO<sub>2</sub>, NMO; k) irradiation; l) deprotection of hydroxyl groups.

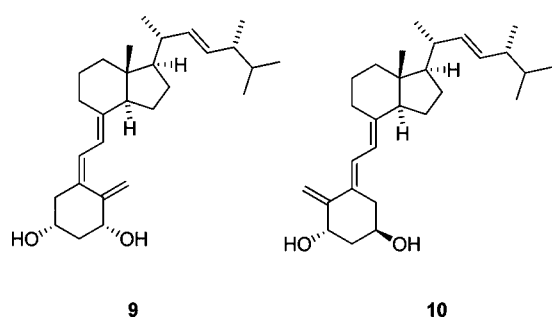


Figure 2. Process impurities observed in the cyclovitamin route.

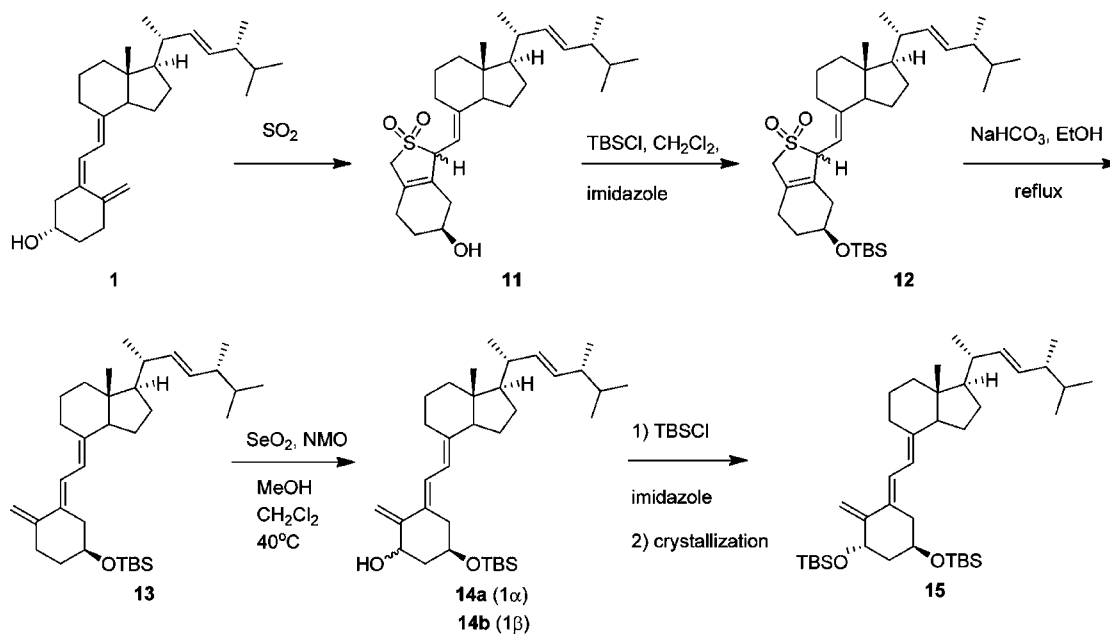
flow processes from the standpoint of scalability, safety, and intensification are well recognized.<sup>13</sup> Flow photoreactors place the reaction solution in close proximity to the light source, and the duration of light exposure can be optimized through the flow rate so as to reduce secondary reactions derived from irradiation of the product. We hypothesized that the greater efficiency of a flow photoreactor would lead to a cleaner reaction that could be scaled beyond the limits of a batch photolysis apparatus.

## RESULTS

Our objective was to use the sulfur dioxide route combined with continuous photoisomerization of the *trans*-triene from the sulfur dioxide route. We also anticipated that careful selection of protecting groups would afford a crystalline intermediate through which we might avoid chromatographic purification. To this end we targeted the crystalline bis-*tert*-butyldimethylsilyl (bis-TBS) ether (15) previously reported by Calverley<sup>14</sup> as the key intermediate (Scheme 2).<sup>15</sup>

Our synthesis of 15 employed a slight modification of Calverley's procedure. Starting from commercially available ergocalciferol (1), the crude intermediates could be taken forward without purification to 15, which was purified by crystallization. Thus, cheletropic cyclization of 1 with excess neat sulfur dioxide at reflux afforded crude sulfone 11 in quantitative yield (Scheme 2). Some SO<sub>2</sub> always remained entrapped in the crude product, even after prolonged pumping under high vacuum. An aqueous NaHCO<sub>3</sub> workup was attempted, but this introduced new colored impurities. However, by calculating the residual SO<sub>2</sub> in the crude product on the basis of the excess crude weight, an adjustment was made to the imidazole charge in the subsequent step, and the crude product (11) was carried forward successfully.

Scheme 2. Synthesis of triene 15 from ergocalciferol



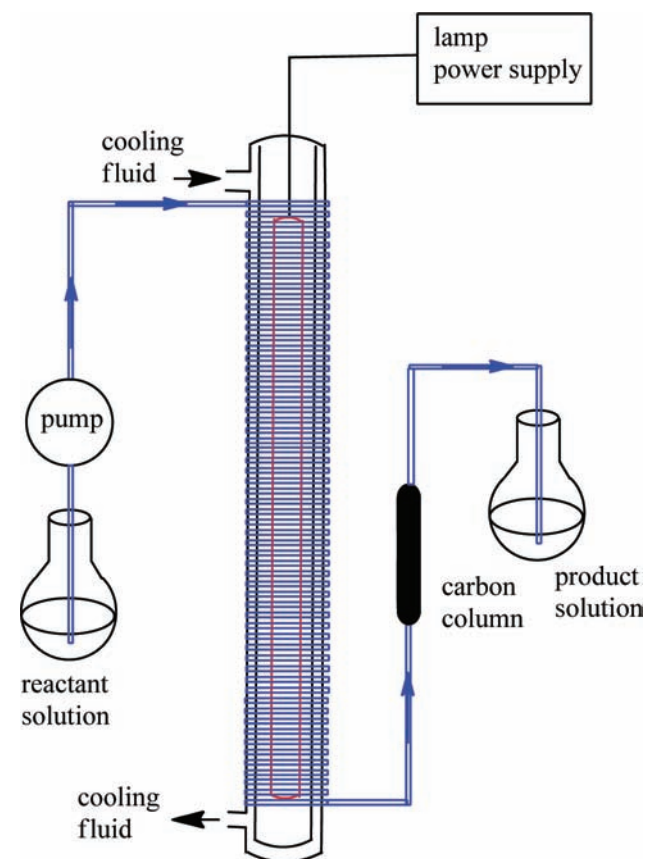
Protection of the carbinol of **11** with a TBS group proceeded smoothly with  $\text{TBSCl}$  and imidazole in dichloromethane to give a 95% yield of **12**. Unacceptably low solubility in ethyl acetate precluded its use in this reaction. The crude, oily silylated sulfone intermediate (**12**) was taken to the next step without purification.

Retrocycloaddition of **12** to afford the (*E,E*)-triene isomer **13** was accomplished by treatment with sodium bicarbonate in anhydrous ethanol at reflux, by analogy with reported procedures.<sup>16</sup> Interestingly, use of 95% ethanol led to a longer reaction time, as did the use of ethyl acetate. Workup consisted of solvent exchange for ethyl acetate, followed by aqueous extraction of the ethyl acetate solution. The resultant oily triene **13** was taken to the next step.

Allylic oxidation of **13** to the alcohol **14** was accomplished with catalytic  $\text{SeO}_2$  and *N*-methylmorpholine-*N*-oxide (NMO) as the stoichiometric oxidant<sup>17</sup> in dichloromethane. The oxidation favored the desired 1 $\alpha$ -isomer (**14a**) over the 1 $\beta$ -isomer (**14b**) with an 85/15 area ratio by HPLC. Attempts to change the reaction solvent to  $\text{EtOAc}$  failed due to poor solubility and slow reaction rate. The crude mixture was taken to the next step. Following a solvent switch to  $\text{EtOAc}$ , TBS protection of the crude isomeric alcohols mixture (**14a/14b**) was accomplished by  $\text{TBSCl}$  with imidazole as base. The crude mixture of *bis*-silyl ethers (**15**) was purified by silica gel filtration followed by two crystallizations from  $\text{MeOH}/\text{EtOAc}$  (2/1 v/v) to afford pure **15** in 20% overall yield from **1**. In addition to removing minor impurities that could complicate the photoisomerization reaction, this purification sequence increased the isomeric C1 ratio from 6:1 to 121:1 ( $\alpha/\beta$ ). As we anticipated, triene **15** was an attractive intermediate for purification owing to its ease of crystallization, stability, and abundant characterization data from the literature, as well as our desire to avoid introduction of photochemically active impurities into the subsequent photoisomerization step.

For the continuous photoisomerization of **15**, we employed an apparatus analogous to that used by Hook et al. in a photocycloaddition reaction (Scheme 3).<sup>11</sup> The assemblage consisted of a PTFE tubing coiled around a photolysis cell,

Scheme 3. Photoisomerization apparatus



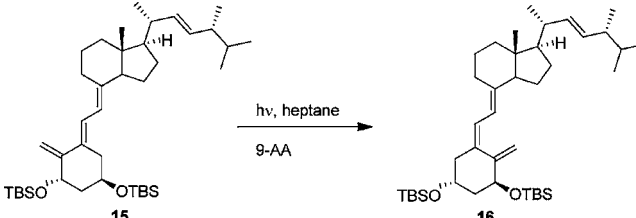
equipped with an immersion well with cooling jacket, a Pyrex sleeve, and a 450 W mercury vapor lamp. The immersion well was connected to a chiller to control the temperature at the interface of the well and tubing. Temperature was monitored with a thermocouple placed between the tubing and the immersion well. The photoisomerization apparatus was wrapped in aluminum foil to contain the light and was further

placed into a safety cabinet. A helium-sparged<sup>18</sup> heptane solution of **15** and a photosensitizer, 9-acetylanthracene (9-AA), was continuously passed via a metering pump through the apparatus into a collection chamber. Both anthracene and 9-AA have been previously reported as required and effective triplet photosensitizers in the photoisomerization of related vitamin D triene systems.<sup>9,19</sup> Starting material and collection flasks were wrapped in foil to avoid fortuitous exposure to light.

Removal of the photosensitizer 9-AA presented a challenge due to its lipophilicity and solubility, which made separation from **16** through crystallization very difficult. However, 9-AA could be effectively removed from the product solution with an in-line, single-use 1:2 carbon/Celite column (3 g mixture per gram of starting material **15**) placed between the photoreactor and the collection vessel.

To our satisfaction, when a heptane solution of **15** (27.5 mg/mL) and 9-AA (10 wt %) was passed through the photoreactor apparatus at a flow rate of 5.5 mL/min at 20 °C, the resultant product solution contained **16** with 96.0% area purity by HPLC, as well as residual **15** (3.21%). Evaporation of the product solution afforded crude **16** in 95% yield. Given this favorable result, we studied the effects of concentration, flow rate, temperature, and 9-AA charge on the HPLC area purity (271 nm detection) of the crude reaction mixture using a full factorial design of experiments (DoE) model including three replicates (runs 4, 7, and 15) at the center point conditions (Table 1).

**Table 1. Four-parameter full factorial experiment in heptane**



run	temp. (°C)	flow rate (mL/min)	conc. ( <b>15</b> ) (mg/mL)	9-AA (wt%)	<b>16</b> (% a/a)	<b>15</b> (% a/a)
1	30	1.9	50.0	4	94.3	4.5
2	30	21.8	50.0	16	90.3	7.1
3	10	21.8	50.0	16	73.8	25.0
4	20	5.5	27.5	10	92.4	6.6
5	30	21.8	5.0	4	95.1	3.9
6	30	1.9	5.0	16	92.6	5.0
7	20	5.5	27.5	10	95.0	4.0
8	10	21.8	5.0	4	96.0	3.1
9	30	1.9	50	16	92.2	6.1
10	10	1.9	50.0	4	95.6	3.5
11	10	21.8	50.0	4	47.1	51.5
12	10	1.9	5.0	16	93.1	5.0
13	10	1.9	5.0	4	91.8	5.4
14	10	21.8	5.0	16	94.7	4.3
15	20	5.5	27.5	10	95.0	4.0
16	30	1.9	5.0	4	92.2	5.2
17	30	21.8	50.0	4	61.9	36.5
18	10	1.9	50.0	16	92.9	5.6
19	30	21.8	5.0	16	92.0	6.7

The design and data analysis were conducted using S-Matrix Fusion Pro software. See Supporting Information for further details.

Using approximately 100 mg per run at the indicated flow rates allowed for individual runs to be conducted and the crude

product to be isolated in a few minutes. For this reason, a full factorial design was selected as opposed to more abbreviated models such as fractional factorial designs. Our initial favorable result was obtained at 20 °C, and the temperature range for the DoE experiment ( $\pm 10$  °C) was set to test robustness about this center point. Concentration and flow rate are both important variables with implications for the throughput of the process on a manufacturing scale, and it was anticipated that these variables would be associated in their effects. For the purpose of the DoE study, wider ranges about the center point settings were thus selected for these variables. A principal concern with the sensitizer range was the ease with which it could be removed from the reaction mixture and a lower charge of this component would be considered preferable; a range of  $\pm 4$  wt % was selected.

Individual runs were generally very clean, with **16** and residual **15** accounting for most of the chromatogram area. Data analysis revealed that the variation in the data was mostly attributable to variable response effects rather than experimental error. Our three center point replicates afforded a standard deviation of 1.50% with 95% confidence limits of  $\pm 6.46$ . The regression analysis using our model had a standard error of  $\pm 0.598$  ( $R^2_{\text{adj}} = 0.693$ ) and  $F = 14.56$  ( $p = 0.0001$ ) (see Supporting Information). Our model was thus appropriate. The model terms are listed in Table 2. Flow rate and concentration

**Table 2. DoE Model terms**

coefficient	model term
2.65	(constant)
0.042	flow rate
0.014	concentration
-0.0032	flow rate * concentration

occur as individual terms with positive coefficients and there is also a mixture term with a negative coefficient containing the product of these two variables. The effect of temperature was relatively constant over the range of 10–30 °C (Figure 3). The relationship between concentration and flow rate was more complex and showed significant curvature (Figure 4). The data suggest that operating at a higher concentration of **15** with lower flow rate, or at lower concentration of **15** with higher flow rate, results in high conversion to **16**. This interaction was anticipated since higher concentration would require longer light exposure and hence a lower flow rate and vice versa. Interestingly, an automated search for the optimal flow rate and concentration revealed a flow rate of 21.8 mL/min and concentration of 5.0 mg/mL, which corresponds to low concentration and high flow rate within the ranges studied (see Supporting Information). The 9-AA sensitizer charge had little effect over the range studied (Figures 5 and 6). The lack of response over the range of sensitizer charges could have several explanations, and although this factor was not studied extensively, further experiments verified that the reaction could be conducted using 2.5 wt % 9-AA, indicating that the original range chosen for the DoE study was probably too narrow.

The photoisomerization reaction worked equally well in ethyl acetate and ethanol. The latter offered the additional advantage of being the solvent in the subsequent deprotection step.

Deprotection of **16** with tetrabutylammonium fluoride in THF, or a combination of THF and either ethyl acetate or heptane, afforded crude doxercalciferol (**3**) that was accompanied

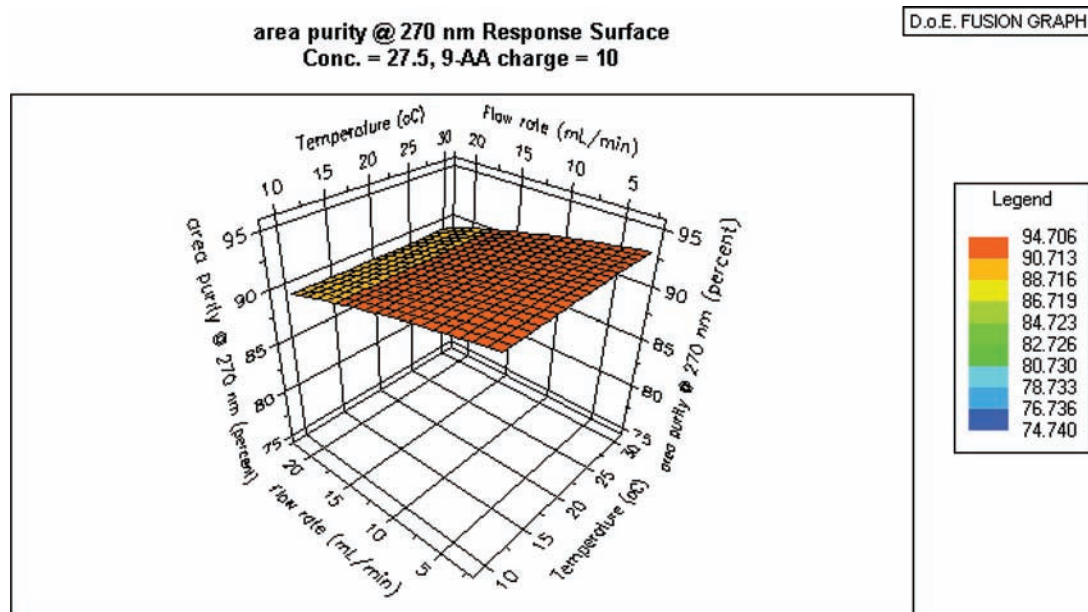


Figure 3. Percent area (16) as a function of temperature and flow rate.

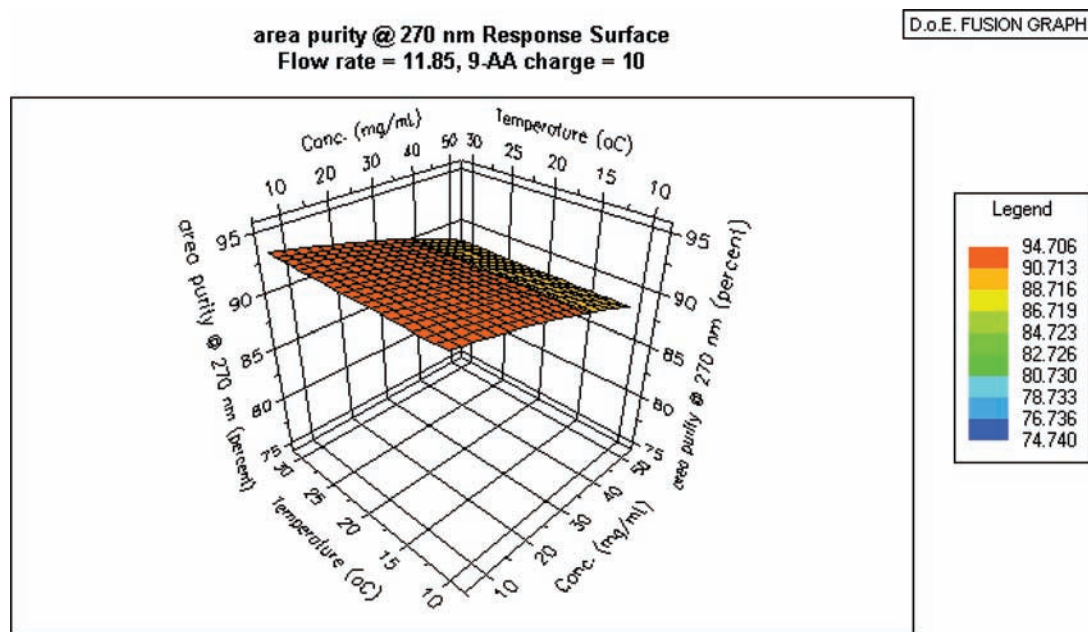


Figure 4. Percent area (16) as a function of temperature and concentration of 15.

by dark-colored impurities which were not characterized. The resultant mixture was not readily purified by crystallization, so an alternative deprotection was explored. Treatment of crude **16** with HCl, generated in situ from acetyl chloride in the presence of an alcohol at room temperature, cleanly afforded crude **3** (Scheme 4).<sup>20</sup>

Purification of crude **3** from the acidic deprotection was possible by crystallization from either methyl formate, methyl formate and ethyl acetate, or isopropyl acetate (Table 3). Using the streamlined photoisomerization in tandem with acidic deprotection and crystallization allowed generation of high-purity doxercalciferol (**3**) without purification of the crude triene (**16**). Notably, the crystallization procedures were efficient in the removal of the isomeric triene impurity (**10**) derived from **15** in the deprotection step.

## CONCLUSION

We developed an improved process for doxercalciferol employing the continuous photoisomerization of a known silylated triene (**15**), which was purified by crystallization. This key triene intermediate was prepared from commercially available ergocalciferol (**1**) in five steps, without purification of intermediates, in an overall yield of about 20%. The photoisomerization of **15** was accomplished using a continuous photoreactor apparatus with inline removal of the photosensitizer (9-AA). The photoisomerization reaction can be run in several solvents at room temperature, but optimal results require careful selection of the flow rate and concentration of **15**. Desilylation of **16** to crude doxercalciferol (**3**) was accomplished with HCl in the presence of alcohol solvent. Purification of the crude product by crystallization afforded

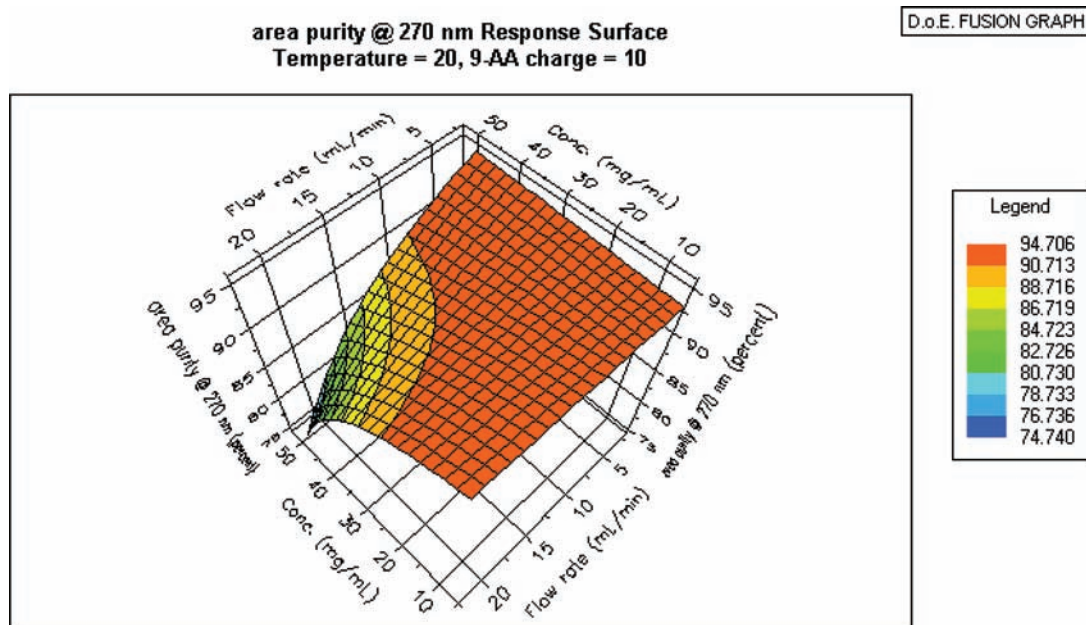


Figure 5. Percent area (16) as a function of flow rate and concentration of 15.

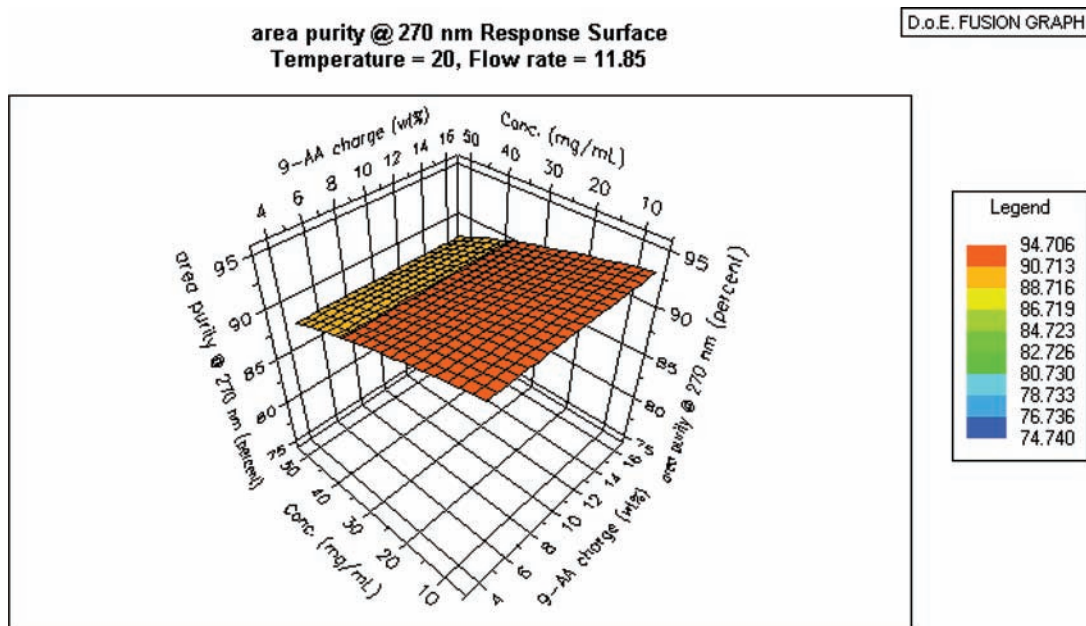
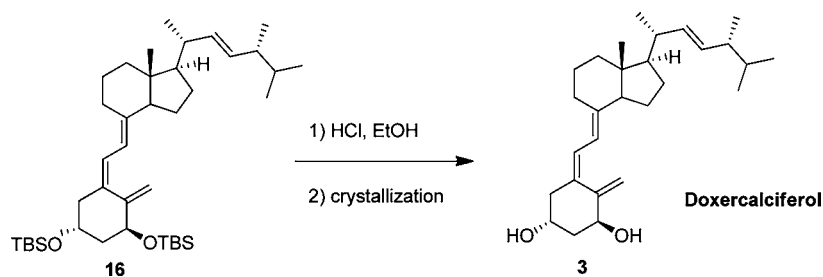


Figure 6. Percent area (16) as a function of concentration and 9-AA charge.

Scheme 4. Deprotection of triene (16) to give doxercalciferol (3) under acidic conditions



high-purity doxercalciferol (3) in about 50% overall yield from 16. Thus, our process can produce doxercalciferol (3) from ergocalciferol in about 10% overall yield without the need

for chromatography. Given the small annual demand for doxercalciferol, the present photochemical isomerization process could be applied using the same photochemical

Table 3. Crystallization of crude doxercalciferol<sup>a</sup>

entry	solvent	3 (%)	10 (%)	yield from 16 (%)
1	methyl formate	99.00	0.58	47
2	methyl formate-EtOAc	99.36	0.06	56
3	<i>i</i> -PrOAc	98.69	0.38	54

<sup>a</sup>Samples were heated to reflux and then cooled to  $-20\text{ }^{\circ}\text{C}$  (see Experimental Section).

apparatus, thus avoiding scale-up-related complications in the key isomerization step. This, combined with the avoidance of chromatography, makes this process an attractive option for manufacturing.

## EXPERIMENTAL SECTION

HPLC data was collected on Waters Alliance 2690 System 600 instruments with PDA detection. HPLC methods were as follows:

**Method A for analysis of compounds 1, 11, 12, 13, 14, 15, 16:** Column: Waters XBridge Phenyl  $3.5\ \mu\text{m}$   $4.6\ \text{mm} \times 150\ \text{mm}$ ; Flow rate:  $1.0\ \text{mL}/\text{min}$ ; Column temperature:  $30\text{ }^{\circ}\text{C}$ ; Detection: photodiode array (see individual chromatograms for wavelength); Gradient elution: (initial)  $10\% \text{H}_2\text{O}/90\% \text{MeOH} \rightarrow (27\ \text{min})\ 5\% \text{H}_2\text{O}/95\% \text{MeOH}$ . Typical retention times (min): **1** (4.86), **11** (3.22), **12** isomers (7.19, 7.55), **13** (12.83), **14a** (6.83), **14b** (7.26), **15** (17.24), **16** (19.78).

**Method B for analysis of compound 3:** Column: Prodigy ODS (3), 100A,  $3\ \mu\text{m}$ ,  $4.6\ \text{mm} \times 150\ \text{mm}$ ; Flow rate:  $1.4\ \text{mL}/\text{min}$ ; Column temperature:  $30\text{ }^{\circ}\text{C}$ ; Detection: 265 nm; Mobile phase:  $\text{H}_2\text{O}/\text{MeCN}$  (1:4 v/v). Typical retention time (min): **3** (19.85).

The photoreactor was assembled as follows: An immersion well apparatus (Ace cat. 7874–35) was connected with flexible tubing to a chiller unit (Lauda-Brinkman RM-6). A 450 W UV lamp (Ace cat. 7825-35) surrounded by a Pyrex sleeve (Ace 7835-44) was inserted into the immersion well. The lamp was attached to a power supply (Ace 7830-60). FEP tubing (Saint-Germain Performance Plastics, AXI00002 Tube,  $0.125''$  (OD)  $\times 0.062''$  ID, 50 ft; VWR cat. 63014-692) was wrapped in a tight, single layer around the immersion well, and aluminum foil was wrapped around the tubing. A KNF STEPDOS liquid pump was attached to the FEP tubing. The inline 1:2 w/w carbon/Celite column (3 g/g starting material) (Ace glass filter column cat. 5813) was placed between the tubing exiting the photoreactor and the collection flask.

DoE analysis was conducted with S-Matrix Fusion Pro software. An automated optimizer using a random walk algorithm beginning from 10 different points on the response surface was employed for optimization searches.

**$\text{SO}_2$ -Cycloadduct of Ergocalciferol (11).** A flask with a dry ice condenser charged with dry ice and isopropanol, a thermocouple, and a magnetic stir bar was assembled. Nitrogen was introduced through a gas inlet adapter and the outlet exhausted through a dry ice and isopropanol cold trap attached to a  $10\% \text{NaOH}$  (aq) scrubber. Solid ergocalciferol (**1**) ( $18.97\ \text{g}$ ,  $47.8\ \text{mmol}$ ) was charged. The tare weight of the flask and stir bar was recorded prior to charging reagents. A dry ice–isopropanol bath ( $\sim -10\text{ }^{\circ}\text{C}$ ) was applied as  $\text{SO}_2$  was slowly introduced with stirring. The solid **1** dissolved during the course of the addition. After 23 min a clear orange solution was achieved as the solid ergocalciferol gradually dissolved, at which time  $\text{SO}_2$  addition was discontinued. The cold bath and condenser were removed, and the residual  $\text{SO}_2$  was allowed to

evaporate under a stream of dry nitrogen. The residue was pumped under high vacuum to further remove  $\text{SO}_2$ . The residual  $\text{SO}_2$  contained in the solid was calculated as follows: The weight of crude **11** was  $24.30\ \text{g}$ , approximately 110% of the theoretical yield ( $22.03\ \text{g}$ ), from which the estimated  $\text{SO}_2$  content of  $2.27\ \text{g}$  ( $35.4\ \text{mmol}$ ) was calculated. The solid was taken directly to the next step.

**$\text{SO}_2$ -Cycloadduct of 3(*S*)-[*tert*-Butyldimethylsilyloxy]-9,10-secoergosta-5,7(*E*),10(19),22(*E*)-tetraene (12).** To the carbinol (**11**) ( $24.30\ \text{g}$ ,  $47.8\ \text{mmol}$ ) under nitrogen was added a suspension of imidazole ( $7.81\ \text{g}$ ,  $115\ \text{mmol}$ ) in  $\text{CH}_2\text{Cl}_2$  ( $132\ \text{mL}$ ), followed by TBSCl ( $8.65\ \text{g}$ ,  $57.4\ \text{mmol}$ ). The solution temperature increased from  $22$  to  $27\text{ }^{\circ}\text{C}$ . After 80 min, additional TBSCl ( $1.44\ \text{g}$ ,  $9.6\ \text{mmol}$ ) was charged. After stirring 165 min, the reaction was 97% complete by HPLC analysis. The solvent was removed by rotary evaporation, and the residue was dissolved in EtOAc ( $200\ \text{mL}$ ) and washed with water ( $100\ \text{mL}$ ) followed by NaCl brine ( $100\ \text{mL}$ ). The EtOAc phase was dried over  $\text{MgSO}_4$  and filtered. Solvent removal afforded crude **12** ( $27.91\ \text{g}$ ). The product was initially an oil, but became a solid at  $-20\text{ }^{\circ}\text{C}$ .

**5(*E*)-Vitamin D<sub>2</sub> TBS Ether (13).** A solution of crude **12** ( $27.49\ \text{g}$ ,  $48\ \text{mmol}$ ),  $95\% \text{EtOH}$  ( $250\ \text{mL}$ ), and  $\text{NaHCO}_3$  ( $25\ \text{g}$ ,  $298\ \text{mmol}$ ) was heated to reflux for 140 min, after which additional  $\text{NaHCO}_3$  ( $5.00\ \text{g}$ ,  $59\ \text{mmol}$ ) was charged, and reflux continued for 2 h. Ethanol was removed by rotary evaporation, then EtOAc was added to the residue to give a milky solution that was filtered to afford a turbid filtrate. The EtOAc phase was washed with water ( $2 \times 100\ \text{mL}$ ) and NaCl brine ( $100\ \text{mL}$ ) and then was dried with  $\text{MgSO}_4$  and filtered. Rotary evaporation afforded crude **13** ( $21.01\ \text{g}$ ,  $41\ \text{mmol}$ ).

**1(*S*),3(*R*)-3-(*tert*-Butyldimethylsilyloxy)-9,10-secoergosta-5(*E*),7(*E*),10(19),22(*E*)-tetraene-1-ol (14).** Powdered  $\text{SeO}_2$  ( $3.19\ \text{g}$ ,  $28.8\ \text{mmol}$ ) was dissolved in MeOH ( $210\ \text{mL}$ ) with sonication. Intermediate **13** ( $21.01\ \text{g}$ ,  $41.1\ \text{mmol}$ ) was charged and dissolved in DCM ( $210\ \text{mL}$ ). To this was added NMO ( $19.3\ \text{g}$ ,  $164\ \text{mmol}$ ), and the mixture was heated to reflux ( $\sim 42\text{ }^{\circ}\text{C}$ ) to give a clear solution. To this refluxing solution was added the methanolic  $\text{SeO}_2$  solution. After 2 h the reaction was cooled to room temperature, and the solvent was rotary evaporated. The residue was dissolved in EtOAc ( $300\ \text{mL}$ ), transferred to a separatory funnel, and washed with water ( $140\ \text{mL}$ ) and then NaCl brine ( $130\ \text{mL}$ ). Both layers had an orange color. The EtOAc phase was dried over  $\text{MgSO}_4$  and filtered. Evaporation afforded the crude carbinol **14** ( $21.67\ \text{g}$ ,  $41.1\ \text{mmol}$ ) as an isomeric mixture (6:1  $\alpha/\beta$  at C1) which was taken to the next step.

**1(*S*),3(*R*)-Bis(*tert*-butyldimethylsilyloxy)-9,10-secoergosta-5(*E*),7(*E*),10(19),22(*E*)-tetraene (15).** Crude carbinol **14** ( $21.60\ \text{g}$ ,  $41.0\ \text{mmol}$ ) was dissolved in  $\text{CH}_2\text{Cl}_2$  ( $110\ \text{g}$ ), and imidazole ( $6.14\ \text{g}$ ,  $90.2\ \text{mmol}$ ) was added. To this was charged TBSCl ( $6.80\ \text{g}$ ,  $45.1\ \text{mmol}$ ) whereupon a precipitate formed. After 195 min, HPLC analysis revealed the reaction was complete. The reaction mixture was dissolved in EtOAc ( $300\ \text{mL}$ ) and washed with water ( $150\ \text{mL}$ ) and then NaCl brine ( $150\ \text{mL}$ ). The EtOAc phase was dried over  $\text{MgSO}_4$  and filtered. Solvent removal afforded **15** ( $25.39\ \text{g}$ ) as a crude foam. A portion of this material was further purified as follows. The foam was dissolved in hexanes ( $13\ \text{mL}/\text{g}$ ) and filtered through a bed of silica gel eluting with  $1\%$  (v/v) EtOAc in hexanes. Solvent was removed by rotary evaporation and high vacuum to give crude **15** ( $1.13\ \text{g}$ ) as a white solid. This was mixed with MeOH and EtOAc ( $2/1\ \text{v/v}$ ,  $34\ \text{mL}$ ) heated at  $61\text{ }^{\circ}\text{C}$ ,

whereupon no solid was present; the mixture was then cooled to 0 °C. After cooling for 55 min, the crystalline solid was suction filtered and washed with cold MeOH and EtOAc (2/1 v/v, 10 mL) and dried overnight at high vacuum to afford **15** (0.61 g, 36:1  $\alpha/\beta$  at C1) as a white solid. This was recrystallized by adding a mixture of MeOH and EtOAc (2/1 v/v, 18.3 mL) and heating to reflux. The clear solution was cooled to room temperature over 20 min and then further cooled in an ice bath for 35 min. The solid was suction filtered, washed with the cold recrystallization solvent (6.1 mL), and dried at room temperature under high vacuum to afford **15** (0.46 g, 0.80 mmol, 121:1  $\alpha/\beta$  at C1). The overall yield from ergocalciferol (**1**) was 20%. <sup>1</sup>H NMR (CDCl<sub>3</sub>)  $\delta$  6.46 (d, 1H, *J* = 11.4), 5.82 (d, 1H, *J* = 11.4), 5.12–5.28 (m, 2H), 4.99 (s, 1H), 4.94 (s, 1H), 4.54 (dd, 1H, *J* = 8.9, 4.0), 4.22 (br s, 1H), 2.87 (d, 1H, *J* = 13.2), 2.55 (dd, 1H, *J* = 14.0, 5.2), 2.32 (d, 1H, *J* = 13.6), 1.81–2.08 (m, 6H), 1.62–1.80 (m, 4H), 1.42–1.53 (m, 3H), 1.23–1.39 (m, 3H), 1.02 (d, 3H, *J* = 6.6), 0.92 (d, 3H, *J* = 6.8), 0.88 (d, 18H, *J* = 16.8), 0.81–0.85 (m, 6H), 0.55 (s, 3H), 0.02–0.10 (m, 12H) ppm.

#### General Procedure for Photoisomerization of **15** to **1(S),3(R)-Bis(tert-butylidimethylsiloxy)-9,10-secoergosta-5(E),7(E),10(19),22(E)-tetraene (16)** for DoE Experiments.

The photoisomerization flow reactor with an inline absorption column was assembled as described above and the lamp turned on prior to adjusting the jacket temperature to the indicated value using the chiller. Triene **15** (105–110 mg) and 9-AA were dissolved in heptane at the indicated concentrations in an amber-colored flask. The solution was sparged with He for at least 5 min prior to being pumped into the reactor. The solution was pumped through the reactor into an amber-colored collection flask. The product (**16**) solution was analyzed by HPLC and concentrated via rotary evaporation to calculate mass recovery.

**Photoisomerization of **15** to **1(S),3(R)-Bis(tert-butylidimethylsiloxy)-9,10-secoergosta-5(E),7(E),10(19),22(E)-tetraene (16)** in Heptane.** A solution of triene **15** (106.2 mg, 0.19 mmol) and 9-AA (14.1 mg, 0.06 mmol) in heptane (20 mL) was sparged with He in an amber flask. The solution was pumped through the flow reactor and the inline 9-AA absorption column at a rate of 21.8 mL/min at 16 °C into an amber collection flask. HPLC analysis of the heptane solution revealed **16** (96.0%, a/a) and residual **15** (3.21%, a/a). Rotary evaporation afforded crude **16** (103 mg, 0.18 mmol) in 95% yield. Proton NMR data were consistent with those reported in the literature.<sup>14</sup> See Supporting Information.

**Photoisomerization of **15** to **1(S),3(R)-Bis(tert-butylidimethylsiloxy)-9,10-secoergosta-5(E),7(E),10(19),22(E)-tetraene (16)** in Ethyl Acetate.** A mixture of **15** (6.17 g, 9.62 mmol) and 9-AA (0.25 g, 1.15 mmol) was dissolved in ethyl acetate (420 mL) to afford a 15 mg/mL solution, and the mixture was sparged with He. The solution was pumped at a rate of 7 mL/min through the photoreactor apparatus as described above. Upon completion (~1 h) the product solution was analyzed by HPLC and found to contain **16** (97.23% a/a) and **10** (2.77% a/a). Rotary evaporation afforded **16** (5.59 g, 8.71 mmol) as a foam in 93% yield.

**Photoisomerization of **15** to **16**, Deprotection, and Crystallization from Methyl Formate to Doxercalciferol (**3**).** An amber vial was charged with triene **15** (0.844 g, 1.48 mmol) followed by 9-AA (31.3 mg, 0.14 mmol, 4 wt %) and EtOAc (60 mL). This solution was passed through the photoisomerization apparatus at a flow rate of 14 mL/min at 20 °C.

HPLC analysis of the product solution showed it to contain **16** in (97.1%, a/a). The solution was rotary evaporated, the residue was dissolved in EtOH (10 mL) and a solution of ethanolic HCl (0.5 mL of 9% v/v 12 N HCl in ethanol) at room temperature. This mixture was stirred overnight at room temperature, at which point HPLC analysis showed complete conversion of **16** to doxercalciferol (**3**). Sodium bicarbonate was added until the pH of the mixture was 7, then the mixture stirred for 1.5 h and filtered. The filtrate was concentrated by rotary evaporation and the residue mixed with methyl formate (7.0 mL) and heated to reflux. The resultant solution was cooled to –20 °C in a freezer for 2 h. The resultant solid was filtered and washed with methyl formate to afford **3** (0.23 g, 0.56 mmol) in 38% yield. The solid was analyzed by HPLC and found to contain **3** (99.09%) and **10** (0.02%). <sup>1</sup>H NMR (CDCl<sub>3</sub>)  $\delta$  6.40 (d, 1H, *J* = 11.2), 6.04 (d, 1H, *J* = 11.2), 5.35 (s, 1H), 5.15–5.29 (m, 2H), 5.03 (s, 1H), 4.45 (dd, 1H, *J* = 7.3, 4.0), 4.21–4.31 (m, 1H), 2.81–2.90 (m, 1H), 2.62 (d, 1H, *J* = 13.3), 2.34 (dd, 1H, *J* = 13.3, 6.5), 1.83–2.11 (m, 6H), 1.42–1.79 (m, 7H), 1.21–1.40 (m, 3H), 1.04 (d, 3H, *J* = 6.6), 0.94 (d, 3H, *J* = 6.8), 0.86 (t, 6H, *J* = 7.3), 0.58 (s, 3H) ppm.

**Alternative Crystallization of Doxercalciferol (**3**) from Methyl Formate and Ethyl Acetate.** Crude **3** (0.71 g, mmol) was combined with methyl formate (14 mL) and heated to reflux. EtOAc (7.0 mL) was gradually added to the refluxing mixture until dissolution was achieved. The mixture was cooled to –20 °C overnight and then was filtered. The resultant solid was dried at room temperature at high vacuum overnight to **3** (0.38 g, 0.92 mmol) in 56% yield. HPLC analysis of this material showed: **3** (99.36%) and **10** (0.06%). HPLC data were consistent with a reference standard. Proton NMR data were consistent with those reported in the literature.<sup>7</sup> See Supporting Information.

**Alternative Crystallization of Doxercalciferol (**3**) from Isopropyl Acetate.** Crude **3** (356 mg) was combined with *i*-PrOAc (10 mL) in a vial and heated to reflux to give a slightly hazy solution. The mixture was cooled to room temperature and stored at –20 °C overnight. The resultant solid was filtered and washed with cold *i*-PrOAc. Drying at room temperature under high vacuum afforded **3** (190 mg, mmol) in 54% yield. HPLC analysis of the resultant solid was as follows: **3** (98.69%, a/a), **10** (0.38% a/a).

## ■ ASSOCIATED CONTENT

### 📄 Supporting Information

DoE experimental details and analysis. NMR spectra of compounds **15** and **3**. This material is available free of charge via the Internet at <http://pubs.acs.org>.

## ■ AUTHOR INFORMATION

### Corresponding Author

william.bauta@genzyme.com

### Present Addresses

<sup>†</sup>Incube Laboratories, 12500 Network Drive, Suite 112, San Antonio, TX 78249.

<sup>‡</sup>307 Laurel Ridge, San Antonio, TX 78253.

### Notes

The authors declare no competing financial interest.



## ACKNOWLEDGMENTS

We thank Dr. Antony Bigot for review of this manuscript and NMR data. We also thank Dr. Leon LeVan and Dr. James Goebel for review and useful discussions.

## REFERENCES

- (1) Holick, M. F. *Vitamin D: Physiology, Molecular Biology, and Clinical Applications*; Springer Verlag: New York, 2009.
- (2) Takeyama, K. I.; Kitanaka, S.; Sato, T.; Kobori, M.; Yanagisawa, J.; Kato, S. *Science* **1997**, *277*, 1827–1830.
- (3) (a) Gravellone, L.; Rizzo, M. A.; Martina, V.; Mezzina, N.; Regalia, A.; Gallieni, M. *Int. J. Nephrol.* **2011**, 1–13. (b) Holick, M. F. *N. Engl. J. Med.* **2007**, *357*, 266–281. (c) Jones, G.; Strugnell, S. A.; DeLuca, H. F. *Physiol. Rev.* **1998**, *78*, 1193–1231.
- (4) (a) Upton, R. A.; Knutson, J. C.; Bishop, C. W.; LeVan, L. W. *Nephrol. Dial. Transplant.* **2003**, *18*, 750–758. (b) Frazao, M.; Chesney, R. W.; Coburn, J. W. *Nephrol. Dial. Transplant.* **1998**, *13* (suppl 3), 68–72. (c) Coburn, J. W.; Tan, A. U.; Levine, B. S.; Mazess, R. B.; Kylo, D. M.; Knutson, J. C.; Bishop, C. W. *Nephrol. Dial. Transplant.* **1996**, *11*, 153–157. (d) Knutson, J. C.; Hollis, B.; LeVan, L. W.; Valliere, C.; Gould, K. G.; Bishop, C. W. *Endocrinology* **1995**, *136*, 4749–4753.
- (5) Zhu, G.-D.; Okamura, W. H. *Chem. Rev.* **1995**, *95*, 1877–1952.
- (6) Paaren, H. E.; Hamer, D. E.; Schnoes, H. K.; DeLuca, H. F. *Proc. Natl. Acad. Sci. U.S.A.* **1978**, *75*, 2080.
- (7) Paaren, H. E.; DeLuca, H. F.; Schnoes, H. K. *J. Org. Chem.* **1980**, *45*, 3253–3258.
- (8) Triene modification through cycloaddition with phthalazine-1,4-dione was employed in the synthesis of 1 $\alpha$ ,25-dihydroxyvitamin D<sub>3</sub>: Andrews, D. R.; Barton, D. H. R.; Hesse, R. H.; Pechet, M. M. *J. Org. Chem.* **1986**, *51*, 4819–4828.
- (9) Gielen, J. W. J.; Koolstra, R. N.; Jacobs, H. J. C.; Havinga, E. *Recl. Trav. Chim. Pays-Bas* **1980**, *99*, 306.
- (10) (a) Bishop, C. W.; Horst, R. L.; Jones, G.; Kozewski, N. J.; Knutson, J. C.; Moriarty, R. M.; Reinhardt, T. A.; Penmasta, R.; Strugnell, S.; Guo, L.; Singhall, S. K.; Zhao, L. U.S. Patent 5,786,348, 1988. (b) Knutson, J. C.; Bishop, C. W.; Moriarty, R. M. U.S. Patent 5,488,120, 1996.
- (11) Hook, B. D. A.; Dohle, W.; Hirst, P. R.; Pickworth, M.; Berry, M. B.; Booker-Milburn, K. I. *J. Org. Chem.* **2005**, *70*, 7558–7564.
- (12) (a) Coyle, E. E.; Oelgemöller, M. *Photochem. Photobiol. Sci.* **2008**, *7*, 1313–1322. (b) Fukuyama, T.; Hino, Y.; Kamata, N.; Ryu, I. *Chem. Lett.* **2004**, *33*, 1430.
- (13) (a) Luis, S. V.; Garcia-Verdugo, E., Eds. *Chemical Reactions and Processes under Flow Conditions*; Royal Society of Chemistry: Cambridge, U.K., 2010. (b) Reay, D.; Ramshaw, C.; Harvey, A. *Process Intensification - Engineering for Efficiency, Sustainability and Flexibility*; Butterworth Heinemann (Elsevier): Burlington, MA, 2008.
- (14) Calverley, M. J. *Tetrahedron* **1987**, *43*, 4609–4619.
- (15) The corresponding *bis-tert*-butyldiphenylsilyl ether has been reported: Shimizu, M.; Ohno, A.; Yamada, S. *Chem. Pharm. Bull.* **2001**, *49*, 312–317.
- (16) (a) Xu, W.-M.; He, J.; Yu, M.-Q.; Shen, G.-X. *Org. Lett.* **2010**, *12*, 4431–4433. (b) Shimizu, M.; Ohno, A.; Yamada, S. *Chem. Pharm. Bull.* **2001**, *49*, 312–317. (c) Manchand, P. S.; Yinnikouros, G. P.; Belica, P. S.; Madan, P. *J. Org. Chem.* **1995**, *60*, 6574–6581.
- (17) Hesse, R. H. U.S. Patent 4,554,105, 1985.
- (18) Helium sparging was conducted as a precaution due to the known photooxidation of vitamin D compounds in solution. See ref 9. Vitamin D is generally unstable in the presence of oxygen. (a) Grady, L. T.; Thakkes, K. D. *J. Pharm. Sci.* **1980**, *69*, 1099–1102. (b) Stewart, B. A.; Midland, S. L.; Byrn, S. R. *J. Pharm. Sci.* **1984**, *73*, 1322–1323.
- (19) (a) Calverley, M. *Tetrahedron Lett.* **1987**, *28*, 1337–1340. (b) Choudhry, H. C.; Belica, P. S.; Coffen, D. L.; Focella, A.; Maehr, H.; Manchand, P. S.; Serico, S.; Yang, R. T. *J. Org. Chem.* **1993**, *58*, 1496–1500. (c) Manchand, P. S.; Yiannikouros, G. P.; Belica, P. S.; Madan, P. *J. Org. Chem.* **1995**, *60*, 6574–6581.
- (20) Nelson, T. D.; Crouch, R. D. *Synthesis* **1996**, 1031–1069.